

Black Hole Production at Future Colliders

Savas Dimopoulos*
Physics Department, Stanford University
Greg Landsberg†
Department of Physics, Brown University

If the scale of quantum gravity is near TeV, the CERN Large Hadron Collider will be producing one black hole (BH) about every second. The decays of the BHs into the final states with prompt, hard photons, electrons, or muons provide a clean signature with low background. The correlation between the BH mass and its temperature, deduced from the energy spectrum of the decay products, can test Hawking's evaporation law and determine the number of large new dimensions and the scale of quantum gravity. We also consider BH production at the proposed future high-energy colliders, such as CLIC and VLHC, and describe the Monte Carlo event generator that can be used to study BH production and decay.

1. Introduction

An exciting consequence of TeV-scale quantum gravity [1, 2, 3] is the possibility of production of black holes (BHs) [4, 5, 6, 7, 8] at the LHC and beyond. This paper summarizes and extends our pioneer work on this subject [7] to the post-LHC future and discusses additional aspects of black-hole phenomenology left out from [7] due to lack of space. Since this work has been completed, numerous follow-up publications on this exciting subject have appeared in the archives, focussing on both the collider [9, 10, 11, 12] and cosmic ray [13, 14, 15] production. We hope that this new branch of phenomenology of extra dimensions will flourish in the months to come, as the black hole production might be the very first evidence for the existence of large extra dimensions.

Black holes are well understood general-relativistic objects when their mass M_{BH} far exceeds the fundamental (higher dimensional) Planck mass $M_P \sim \text{TeV}$. As M_{BH} approaches M_P , the BHs become “stringy” and their properties complex. In what follows, we will ignore this obstacle and estimate the properties of light BHs by simple semiclassical arguments, strictly valid for $M_{\text{BH}} \gg M_P$. We expect that this will be an adequate approximation, since the important experimental signatures rely on two simple qualitative properties: (i) the absence of small couplings and (ii) the “democratic” nature of BH decays, both of which may survive as average properties of the light descendants of BHs. Nevertheless, because of the unknown stringy corrections, our results are approximate estimates. For this reason, we will not attempt selective partial improvements—such as time dependence, angular momentum, charge, hair, and other higher-order general relativistic refinements—which, for light BHs, may be masked by larger unknown stringy effects. We will focus on the production and sudden decay of Schwarzschild black holes.

2. Production

The Schwarzschild radius R_S of an $(4 + n)$ -dimensional black hole is given by [16], assuming that extra dimensions are large ($\gg R_S$).

Consider two partons with the center-of-mass (c.o.m.) energy $\sqrt{\hat{s}} = M_{\text{BH}}$ moving in opposite directions. Semiclassical reasoning suggests that if the impact parameter is less than the (higher dimensional) Schwarzschild radius, a BH with the mass M_{BH} forms. Therefore the total cross

*E-mail: savas@leland.stanford.edu

†E-mail: landsberg@hep.brown.edu

section can be estimated from geometrical arguments [17], and is of order

$$\sigma(M_{\text{BH}}) \approx \pi R_S^2 = \frac{1}{M_P^2} \left[\frac{M_{\text{BH}}}{M_P} \left(\frac{8\Gamma\left(\frac{n+3}{2}\right)}{n+2} \right) \right]^{\frac{2}{n+1}}$$

(see Figure 1a,d) [18].

This expression contains no small coupling constants; if the parton c.o.m. energy $\sqrt{\hat{s}}$ reaches the fundamental Planck scale $M_P \sim \text{TeV}$ then the cross section is of order $\text{TeV}^{-2} \approx 400 \text{ pb}$. At the LHC or VLHC, with the total c.o.m. energy $\sqrt{s} = 14 \text{ TeV}$ or $100\text{-}200 \text{ TeV}$, respectively, BHs will be produced copiously. To calculate total production cross section, we need to take into account that only a fraction of the total c.o.m. energy in a pp collision is achieved in a parton-parton scattering. We compute the full particle level cross section using the parton luminosity approach (see, e.g., Ref. [19]):

$$\frac{d\sigma(pp \rightarrow \text{BH} + X)}{dM_{\text{BH}}} = \frac{dL}{dM_{\text{BH}}} \hat{\sigma}(ab \rightarrow \text{BH}) \Big|_{\hat{s}=M_{\text{BH}}^2},$$

where the parton luminosity dL/dM_{BH} is defined as the sum over all the initial parton types:

$$\frac{dL}{dM_{\text{BH}}} = \frac{2M_{\text{BH}}}{s} \sum_{a,b} \int_{M_{\text{BH}}^2/s}^1 \frac{dx_a}{x_a} f_a(x_a) f_b\left(\frac{M_{\text{BH}}^2}{sx_a}\right),$$

and $f_i(x_i)$ are the parton distribution functions (PDFs). We used the MRSD-' [20] PDF set with the Q^2 scale taken to be equal to M_{BH} [21], which is within the allowed range for this PDF set, up to the VLHC kinematic limit. Cross section dependence on the choice of PDF is $\approx 10\%$.

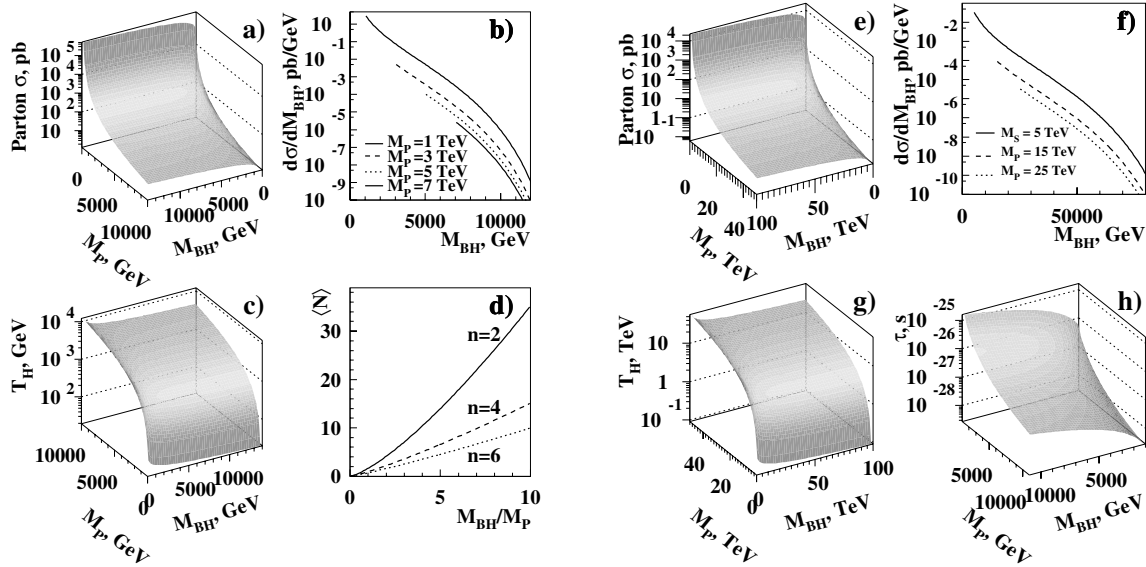


Figure 1: Black-hole properties at the LHC a)-d),h) and VLHC d)-h). a,e) Parton-level production cross section; b,f) differential cross section $d\sigma/dM_{\text{BH}}$; c,g) Hawking temperature; d) average decay multiplicity for a Schwarzschild black hole; and h) black-hole lifetime. The number of extra spatial dimensions $n = 4$ is used for a)-c), e)-h). The dependence of the cross section and the Hawking temperature on n is weak and would be hardly noticeable on the logarithmic scale. The lifetime drops by about two orders of magnitude for n increase from 2 to 7.

The differential cross sections $d\sigma/dM_{\text{BH}}$ for the BH produced at the LHC and a 200 TeV VLHC machines are shown in Figs. 1b and 1f, respectively, for several choices of M_P . The total production cross section at the LHC for BH masses above M_P ranges from 0.5 nb for $M_P = 2 \text{ TeV}$, $n = 7$ to 120 fb for $M_P = 6 \text{ TeV}$ and $n = 3$. If the fundamental Planck scale is $\approx 1 \text{ TeV}$, LHC, with the peak luminosity of $30 \text{ fb}^{-1}/\text{year}$ will produce over 10^7 black holes per year. This is comparable to the total number of Z 's produced at LEP, and suggests that we may do high precision studies

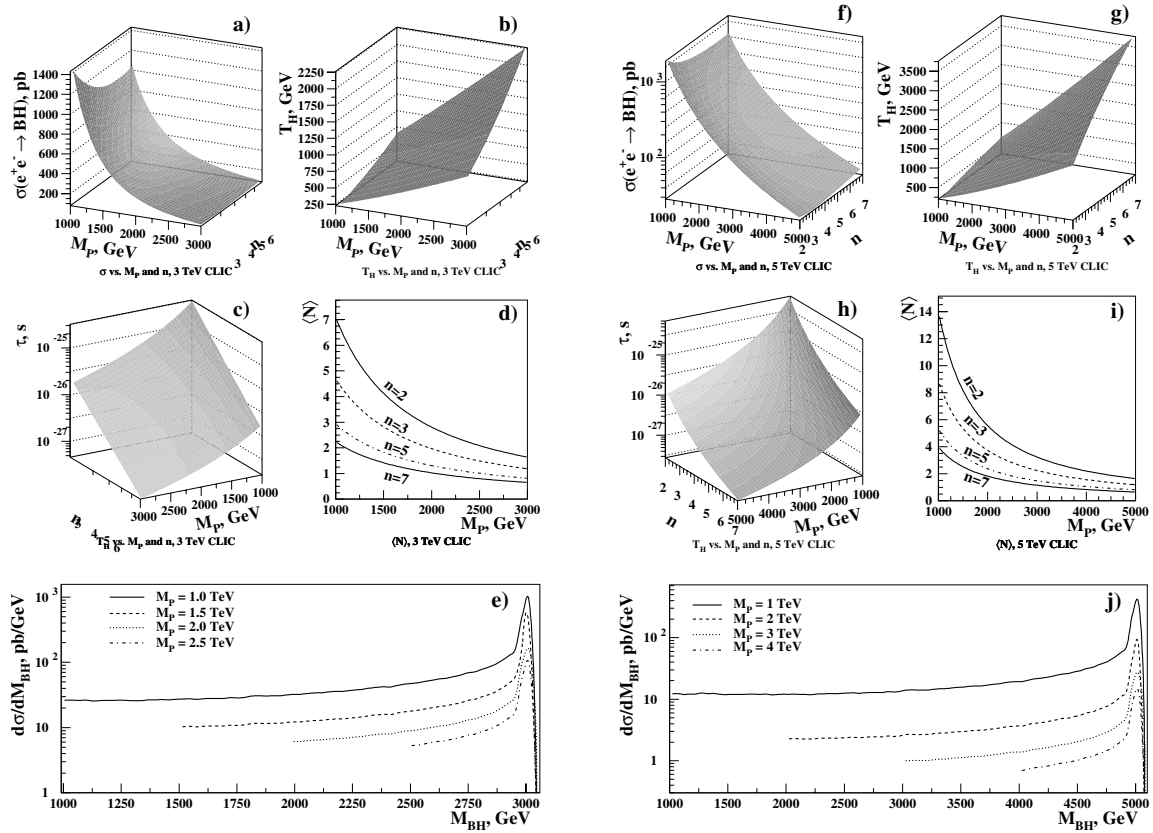


Figure 2: Black hole properties at high-energy lepton colliders. Plots a)–d) and f)–i) correspond to the properties (production cross-section, temperature, lifetime, and average decay multiplicity) of a fixed-mass 3 TeV and 5 TeV black hole produced at a 3 TeV or a 5 TeV machine, respectively. Plots e), j) show the differential cross section of BH production for $n = 4$, as a function of the BH mass at a 3 TeV or a 5 TeV CLIC e^+e^- -collider, respectively.

of TeV BH physics, as long as the backgrounds are kept small. At the VLHC, BHs will be produced copiously for their masses and the value of the fundamental Planck scale as high as 25 TeV. The total production cross section is of the order of a millibarn for $M_P = 1$ TeV and of a picobarn for $M_P = 25$ TeV.

Similarly, the black holes can be produced at future high-energy lepton colliders, such as CLIC or a muon collider. To a first approximation, such a machine produces black holes of a fixed mass, equal to the energy of the machine. The total cross section of such a BH produced at a 3 TeV and a 5 TeV machine, as a function of M_P and n , is shown in Fig 2a and Figure 2f, respectively. For more elaborated studies of the BH production at electron colliders, one should take into account machine *beamstrahlung*. The beamstrahlung-corrected energy spectrum of the machine plays the same role as the parton luminosity at a hadron collider, except that for the e^+e^- machine it is peaked at the nominal machine energy, rather than at small values of \sqrt{s} , characteristic of a hadron collider. Using typical beamstrahlung spectra expected for a 3 TeV or a 5 TeV CLIC machine, we show the differential cross section $d\sigma/dM_{\text{BH}}$ of the black hole production at a 3 and a 5 TeV CLIC in Figure 2e and Figure 2j, respectively.

3. Decay

The decay of the BH is governed by its Hawking temperature T_H , which is proportional to the inverse radius, and given by [16]:

$$T_H = M_P \left(\frac{M_P}{M_{\text{BH}}} \frac{n+2}{8\Gamma\left(\frac{n+3}{2}\right)} \right)^{\frac{1}{n+1}} \frac{n+1}{4\sqrt{\pi}} = \frac{n+1}{4\pi R_S} \quad (1)$$

(see Figs. 1c,g and 2b,g). As the collision energy increases, the resulting BH gets heavier and its decay products get colder.

Note that the wavelength $\lambda = \frac{2\pi}{T_H}$ corresponding to the Hawking temperature is larger than the size of the black hole. Therefore, the BH acts as a point-radiator and emits mostly s -waves. This indicates that it decays equally to a particle on the brane and in the bulk, since it is only sensitive to the radial coordinate and does not make use of the extra angular modes available in the bulk. Since there are many more particles on our brane than in the bulk, this has the crucial consequence that the BH decays visibly to standard model (SM) particles [6, 22].

The average multiplicity of particles produced in the process of BH evaporation is given by: $\langle N \rangle = \left\langle \frac{M_{\text{BH}}}{E} \right\rangle$, where E is the energy spectrum of the decay products. In order to find $\langle N \rangle$, we note that the BH evaporation is a blackbody radiation process, with the energy flux per unit of time given by Planck's formula: $\frac{df}{dx} \sim \frac{x^3}{e^{x+c}}$, where $x \equiv E/T_H$, and c is a constant, which depends on the quantum statistics of the decay products ($c = -1$ for bosons, $+1$ for fermions, and 0 for Boltzmann statistics).

The spectrum of the BH decay products in the massless particle approximation is given by: $\frac{dN}{dE} \sim \frac{1}{E} \frac{df}{dE} \sim \frac{x^2}{e^{x+c}}$. For averaging the multiplicity, we use the average of the distribution in the inverse particle energy:

$$\left\langle \frac{1}{E} \right\rangle = \frac{1}{T_H} \frac{\int_0^\infty dx \frac{1}{x} \frac{x^2}{e^{x+c}}}{\int_0^\infty dx \frac{x^2}{e^{x+c}}} = a/T_H, \quad (2)$$

where a is a dimensionless constant that depends on the type of produced particles and numerically equals 0.68 for bosons, 0.46 for fermions, and $\frac{1}{2}$ for Boltzmann statistics. Since a mixture of fermions and bosons is produced in the BH decay, we can approximate the average by using Boltzmann statistics, which gives the following formula for the average multiplicity: $\langle N \rangle \approx \frac{M_{\text{BH}}}{2T_H}$. Using Eq. (1) for Hawking temperature, we obtain:

$$\langle N \rangle = \frac{2\sqrt{\pi}}{n+1} \left(\frac{M_{\text{BH}}}{M_P} \right)^{\frac{n+2}{n+1}} \left(\frac{8\Gamma\left(\frac{n+3}{2}\right)}{n+2} \right)^{\frac{1}{n+1}} \quad (3)$$

Eq. (3) holds for $M_{\text{BH}} \gg T_H$, i.e. $\langle N \rangle \gg 1$; otherwise, the Planck spectrum is truncated at $E \approx M_{\text{BH}}/2$ by the decay kinematics [23]. The average number of particles produced in the process of BH evaporation is shown in Figs. 1d and 2d,i.

The lifetime of the BH can be estimated by using the Stefan's law of thermal radiation. Since BH evaporation occurs primarily in three spatial dimensions, the canonical 3-dimensional Stefan's law applies, and therefore the power dissipated by the Hawking's radiation per unit area of the BH event horizon is $p = \sigma T_H^4$, where σ is the Stefan-Boltzmann constant and T_H is the Hawking temperature of the BH. Since the effective evaporation area of the BH is the area of a 3-dimensional sphere with the radius equal to the BH Schwarzschild radius R_S , the total power dissipated by the BH is given by:

$$P = 4\pi R_S^2 p = 4\pi R_S^2 \sigma T_H^4 = \sigma T_H^2 \frac{(n+1)^2}{4\pi}.$$

The BH lifetime τ is given by:

$$\tau = M_{\text{BH}}/P = \frac{4\pi M_{\text{BH}}}{\sigma T_H^2 (n+1)^2},$$

and using Eq. (1), as well as the expression for σ in natural units ($\hbar = c = k = 1$), $\sigma = \pi^2/60$ [24], we find:

$$\tau = \frac{3840}{M_p(n+1)^4} \left(\frac{M_{\text{BH}}}{M_p} \right)^{\frac{n+3}{n+1}} \left(\frac{8\Gamma\left(\frac{n+3}{2}\right)}{n+2} \right)^{\frac{2}{n+1}}.$$

The lifetime of a black hole as a function of its mass and the fundamental Planck scale is shown in Figs. 1h and 2c,h. A typical lifetime of a BH is $\sim 10^{-26}$ s, which corresponds to a rather narrow width of the BH state ~ 10 GeV, i.e. typical for, e.g., a W' or Z' resonance of a similar mass.

We emphasize that, throughout this paper, we ignore time evolution: as the BH decays, it gets lighter and hotter and its decay accelerates. We adopt the “sudden approximation” in which the BH decays, at its original temperature, into its decay products. This approximation should be reliable as the BH spends most of its time near its original mass and temperature, because that is when it evolves the slowest; furthermore, that is also when it emits the most particles. Later, when we test the Hawking’s mass-temperature relation by reconstructing Wien’s displacement law, we will minimize the sensitivity to the late and hot stages of the BHs life by looking at only the soft part of the decay spectrum. Proper treatment of time evolution, for $M_{\text{BH}} \approx M_p$, is difficult, since it immediately takes us to the stringy regime.

4. Branching Fractions

The decay of a BH is thermal: it obeys all local conservation laws, but otherwise does not discriminate between particle species (of the same mass and spin). Theories with quantum gravity near a TeV must have additional symmetries, beyond the standard $SU(3) \times SU(2) \times U(1)$, to guarantee proton longevity, approximate lepton number(s) and flavor conservation [25]. There are many possibilities: discrete or continuous symmetries, four dimensional or higher dimensional “bulk” symmetries [26]. Each of these possible symmetries constrains the decays of the black holes. Since the typical decay involves a large number of particles, we will ignore the constraints imposed by the few conservation laws and assume that the BH decays with roughly equal probability to all off ≈ 60 particles of the SM. Since there are six charged leptons and one photon, we expect $\sim 10\%$ of the particles to be hard, primary leptons and $\sim 2\%$ of the particles to be hard photons, each carrying hundreds of GeV of energy. This is a very clean signal, with negligible background, as the production of SM leptons or photons in high-multiplicity events at the LHC occurs at a much smaller rate than the BH production (see Figure 3). These events are also easy to trigger on, since they contain at least one prompt lepton or photon with the energy above 100 GeV, as well as energetic jets.

5. Test of Hawking Radiation

Furthermore, since there are three neutrinos, we expect only $\sim 5\%$ average missing transverse energy (\cancel{E}_T) per event, which allows us to precisely estimate the BH mass from the visible decay products. We can also reconstruct the BH temperature by fitting the energy spectrum of the decay products to the Planck’s formula. Simultaneous knowledge of the BH mass and its temperature allows for a test of the Hawking radiation and can provide an evidence that the observed events come from the production of BH, and not from some other new physics.

There are a few important experimental techniques that we will use to carry out the numerical test. First of all, to improve precision of the BH mass reconstruction we will use only the events with \cancel{E}_T consistent with zero. Given the small probability for a BH to emit a neutrino or a graviton, total statistics won’t suffer appreciably from this requirement. Since BH decays have large jet activity, the M_{BH} resolution will be dominated by the jet energy resolution and the initial state radiation effects, and is expected to be ~ 100 GeV for a massive BH. Second, we will use only photons and electrons in the final state to reconstruct the Hawking temperature. The reason is twofold: final states with energetic electrons and photons have very low background at high \sqrt{s} , and the energy resolution for electrons and photons remains excellent even at the highest energies achieved in the process of BH evaporation. We do not use muons, as their momenta are determined by the track curvature in the magnetic field, and thus the resolution deteriorates fast

with the muon momentum growth. We also ignore the τ -lepton decay modes, as the final states with τ 's have much higher background than inclusive electron or photon final states, and also because their energies can not be reconstructed as well as those for the electromagnetic objects. Fraction of electrons and photons among the final state particles is only $\sim 5\%$, but the vast amount of BHs produced at the LHC allows us to sacrifice the rest of the statistics to allow for a high-precision measurement. (Also, the large number of decay particles enhances the probability to have a photon or an electron in the event.) Finally, if the energy of a decay particle approaches the kinematic limit for pair production, $M_{\text{BH}}/2$, the shape of the energy spectrum depends on the details of the BH decay model. In order to eliminate this unwanted model dependence, we use only the low part of the energy spectrum with $E < M_{\text{BH}}/2$.

The experimental procedure is straightforward: we select the BH sample by requiring events with high mass (> 1 TeV) and multiplicity of the final state ($N \geq 4$), which contain electrons or photons with energy > 100 GeV. We smear the energies of the decay products with the resolutions typical of the LHC detectors. We bin the events in the invariant mass with the bin size (500 GeV) much wider than the mass resolution. The mass spectrum of the BHs produced at the LHC with 100 fb^{-1} of integrated luminosity is shown in Figure 3 for several values of M_P and n . Backgrounds from the SM $Z(ee) + \text{jets}$ and $\gamma + \text{jets}$ production, as estimated with PYTHIA [27], are small (see Figure 3).

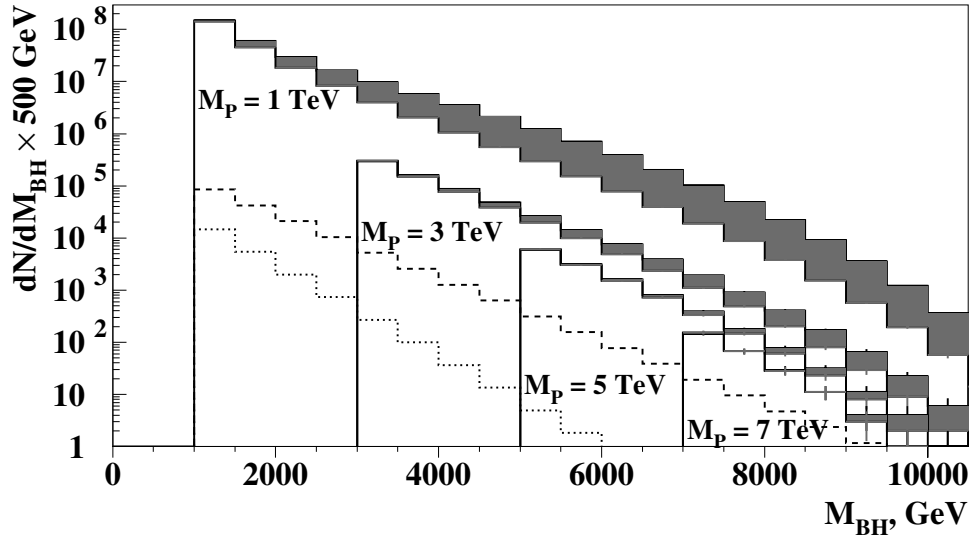


Figure 3: Number of BHs produced at the LHC in the electron or photon decay channels, with 100 fb^{-1} of integrated luminosity, as a function of the BH mass. The shaded regions correspond to the variation in the number of events for n between 2 and 7. The dashed line shows total SM background (from inclusive $Z(ee)$ and direct photon production). The dotted line corresponds to the $Z(ee) + X$ background alone.

To determine the Hawking temperature as a function of the BH mass, we perform a maximum likelihood fit of the energy spectrum of electrons and photons in the BH events to the Planck's formula (with the coefficient c determined by the particle spin), below the kinematic cutoff ($M_{\text{BH}}/2$). This fit is performed using the entire set of the BH events (i.e., not on the event-by-event basis), separately in each of the M_{BH} bins. We then use the measured M_{BH} vs. T_H dependence and Eq. (1) to determine the fundamental Planck scale M_P and the dimensionality of space n . Note that to determine n we can also take the logarithm of both sides of Eq. (1):

$$\log(T_H) = \frac{-1}{n+1} \log(M_{\text{BH}}) + \text{const}, \quad (4)$$

where the constant does not depend on the BH mass, but only on M_P and on detailed properties of the bulk space, such as shape of extra dimensions. Therefore, the slope of a straight-line fit to the $\log(T_H)$ vs. $\log(M_{\text{BH}})$ data offers a direct way of determining the dimensionality of space. This is a multidimensional analog of Wien's displacement law. Note that Eq. (4) is fundamentally different from other ways of determining the dimensionality of space-time, e.g. by studying a

monojet signature or a virtual graviton exchange processes, also predicted by theories with large extra dimensions. (The properties of the latter two processes always depend on the volume of the extra-dimensional space, i.e. they cannot yield information on the number of extra dimensions without specific assumptions on their relative size.)

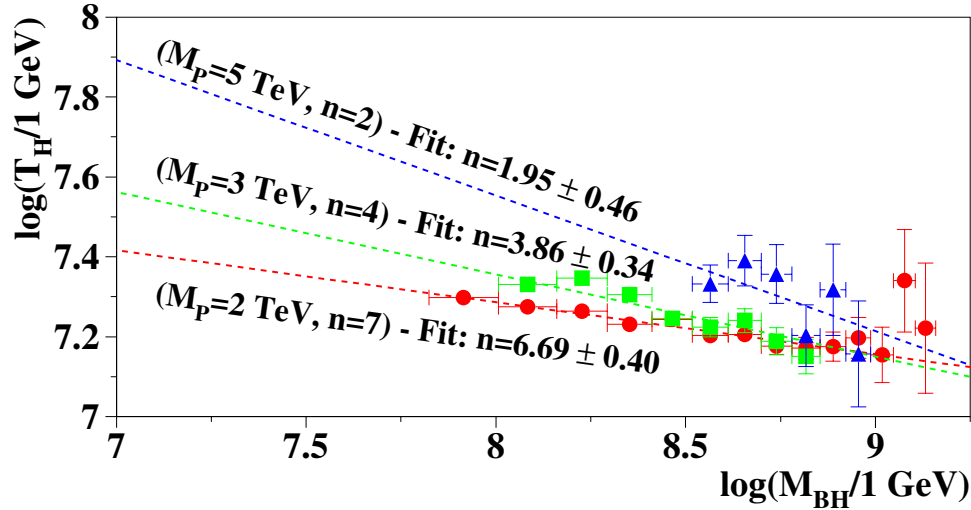


Figure 4: Determination of the dimensionality of space via Wien's displacement law at the LHC with 100 fb^{-1} of data.

Test of the Wien's law at the LHC would provide a confirmation that the observed $e + X$ and $\gamma + X$ event excess is due to the BH production. It would also be the first experimental test of the Hawking's radiation hypothesis. Figure 4 shows typical fits to the simulated BH data at the LHC, corresponding to 100 fb^{-1} of integrated luminosity, for the highest fundamental Planck scales that still allow for determination of the dimensionality of space with reasonable precision. The reach of the LHC for the fundamental Planck scale and the number of extra dimensions via Hawking radiation extends to $M_P \sim 5 \text{ TeV}$ and is summarized in Table 5 [28].

Similar tests can be performed at the VLHC and CLIC machines. While the VLHC case is identical to that at the LHC, with appropriately scaled energies, CLIC is complementary to the LHC in many ways, as the maximum number of BH produced at CLIC is found at the highest accessible masses. This gives certain advantage, as the stringy effects, as well as kinematic distortion of the Planck black-body spectrum decrease with the increase of the BH mass. Thus the M_{BH} vs. T_H fit at CLIC is less affected by these unknown effects. Preliminary studies show that statistical sensitivity to the number of extra dimensions and the value of the fundamental Planck scale at CLIC is similar to that at the LHC.

Table I Determination of M_P and n from Hawking radiation. The two numbers in each column correspond to fractional uncertainty in M_P and absolute uncertainty in n , respectively.

M_P	1 TeV	2 TeV	3 TeV	4 TeV	5 TeV
$n = 2$	1%/0.01	1%/0.02	3.3%/0.10	16%/0.35	40%/0.46
$n = 3$	1%/0.01	1.4%/0.06	7.5%/0.22	30%/1.0	48%/1.2
$n = 4$	1%/0.01	2.3%/0.13	9.5%/0.34	35%/1.5	54%/2.0
$n = 5$	1%/0.02	3.2%/0.23	17%/1.1		
$n = 6$	1%/0.03	4.2%/0.34	23%/2.5	Fit fails	
$n = 7$	1%/0.07	4.5%/0.40	24%/3.8		

Note, that the BH discovery potential at the LHC and VLHC is maximized in the $e/\mu + X$ channels, where background is much smaller than that in the $\gamma + X$ channel (see Figure 3). The reach of a simple counting experiment extends up to $M_P \approx 9 \text{ TeV}$ at the LHC and $M_P \approx 50 \text{ TeV}$ at the VLHC ($n = 2-7$), where one would expect to see a handful of BH events with negligible background.

6. Black Hole Monte Carlo Event Generator

A Monte Carlo package, TRUENOIR, has been developed for simulating production and decay of the black holes at high-energy colliders. This package is a plug-in module for the PYTHIA [27] Monte Carlo generator. It uses a heuristic algorithm and conservation of baryon and lepton numbers, as well as the QCD color, to simulate the decay of a black hole in a rapid-decay approximation. While the limitations of such a simplistic approach are clear, further improvements to this generator are being worked on. In the meantime, it provides a useful qualitative tool to study the detector effects and other aspects of the BH event reconstruction. Figure 5 shows a display of a typical BH event at a 5 TeV CLIC collider, produced using the TRUENOIR code. A characteristic feature of this event is extremely large final state multiplicity, very atypical of the events produced in e^+e^- collisions.

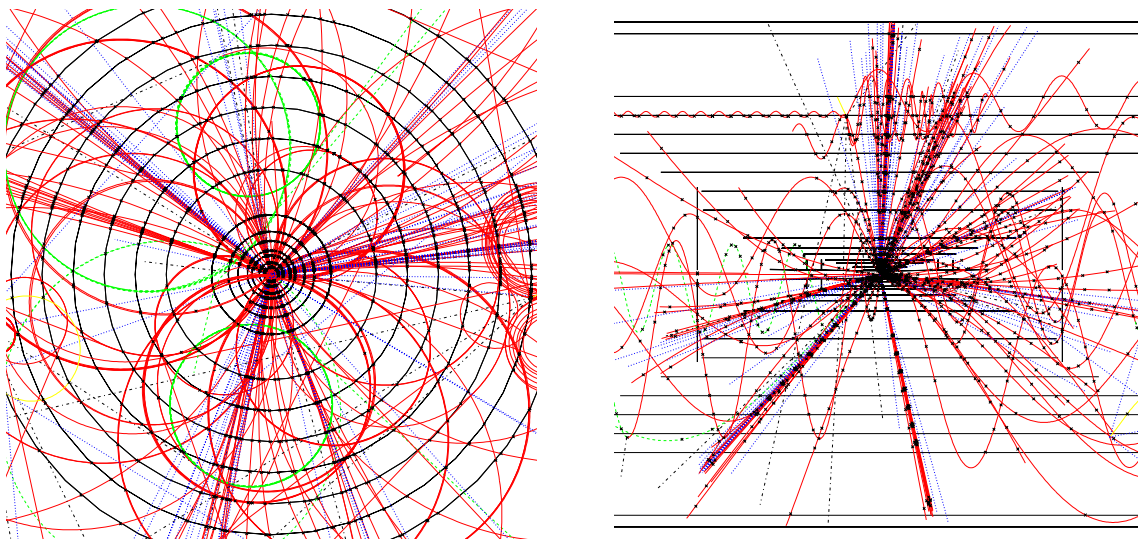


Figure 5: A typical black-hole event at a 5 TeV CLIC accelerator. The two views correspond to the end and side-views of a CLIC detector. Detector simulation by Albert De Roeck.

7. Summary

Black hole production at the LHC and beyond may be one of the early signatures of TeV-scale quantum gravity. It has three advantages:

- (i) Large Cross Section: No small dimensionless coupling constants, analogous to α , suppress the production of BHs. This leads to enormous rates.
- (ii) Hard, Prompt, Charged Leptons and Photons: Thermal decays are flavor-blind. This signature has practically vanishing SM background.
- (iii) Little Missing Energy: This facilitates the determination of the mass and the temperature of the black hole, and may lead to a test of Hawking radiation.

It is desirable to improve our primitive estimates, especially for the light black holes ($M_{\text{BH}} \sim M_P$); this will involve string theory. Nevertheless, the most telling signatures of BH production—large and growing cross sections; hard leptons, photons, and jets—emerge from qualitative features that are expected to be reliably estimated from the semiclassical arguments of this paper.

Perhaps black holes will be the first signal of TeV-scale quantum gravity. This depends on, among other factors, the relative magnitude of M_P and the (smaller) string scale M_S . For $M_S \ll M_P$, the vibrational modes of the string may be the first indication of the new physics.

Studies of the BH properties at future facilities, including very high-energy lepton and hadron colliders would allow to map out properties of large extra dimensions, measure the effects of

quantum gravity, and to provide insight into other quantum phenomena, such as Hawking radiation, information paradox, etc.

Acknowledgments

We would like to thank Gia Dvali, Veronika Hubeny, Nemanja Kaloper, Elias Kiritsis, Joe Lykken, Konstantin Matchev, Steve Mrenna, and Lenny Susskind for valuable conversations. This work was partially supported by the U.S. DOE Grant No. DE-FG02-91ER40688, NSF Grant No. PHY-9870115, and A.P. Sloan Foundation.

References

- [1] N. Arkani-Hamed, S. Dimopoulos, and G. Dvali, Phys. Lett. **B429**, 263 (1998), hep-th/9803315.
- [2] I. Antoniadis, N. Arkani-Hamed, S. Dimopoulos, and G. Dvali, Phys. Lett. **B436**, 257 (1998), hep-th/9804398.
- [3] N. Arkani-Hamed, S. Dimopoulos, and G. Dvali, Phys. Rev. D **59**, 086004 (1999), hep-th/9807344.
- [4] P. Argyres, S. Dimopoulos, and J. March-Russell, Phys. Lett. **B441**, 96 (1998), hep-th/9808138.
- [5] (1999), hep-th/9906038.
- [6] R. Emparan, G. Horowitz, and R. Myers, Phys. Rev. Lett. **85**, 499 (2000), hep-th/0003118.
- [7] S. Dimopoulos and G. Landsberg, Phys. Rev. Lett. **87**, 106295 (2001), hep-th/0106295.
- [8] (2001), hep-ph/0106219v3.
- [9] M. Voloshin, Phys. Lett. **B518**, 137 (2001), hep-ph/0107019.
- [10] (2001), hep-ph/0108060.
- [11] (2001), hep-ph/0109085.
- [12] (2001), hep-ph/0110163.
- [13] (2001), hep-ph/0109106.
- [14] (2001), hep-ph/0109242.
- [15] (2001), hep-ph/0109287.
- [16] R. Myers and M. Perry, Ann. Phys. **172**, 304 (1986).
- [17] In fact the cross section is somewhat enhanced by initial-state attraction [6].
- [18] Exponential suppression of the BH production, claimed in [9] is not applicable to this work, as the BH collapse is due to a classical evolution, rather than tunneling. This was confirmed by, e.g., the analysis in Ref. [10].
- [19] E. Eichten, I. Hinchliffe, K. Lane, and C. Quigg, Rev. Mod. Phys. **56**, 579 (1984).
- [20] A. Martin, R. Roberts, and W. Stirling, Phys. Lett. **B306**, 145 (1993).
- [21] While another choice of $Q^2 = 1/R_S^2$, as used, e.g., in [8], is also a logical possibility, we choose to use a more conservative assumption, as the actual relevant scale depends on unknown stringy effects, and likely to be somewhere between these two extremes.
- [22] p. c. L. Susskind.
- [23] To avoid this limitation when performing numerical tests of Wien's law, we truncate the integrals in Eq. (2) at the kinematic limit ($M_{\text{BH}}/2$).
- [24] In the above calculations we used the Stefan-Boltzmann constant, which is strictly speaking correct only for an evaporation via massless bosons. However, since the nature of our calculations is very approximate, this is a reasonable assumption.
- [25] Any form of new physics at a TeV requires such new symmetries (e.g., R-parity for TeV-scale SUSY).
- [26] (1998), hep-ph/9811353.
- [27] T. Sjöstrand, Comp. Phys. Comm. **82**, 74 (1994).
- [28] We checked the effect of introducing an additional cutoff at $E < M_S$, where string dynamics is expected to affect the shape of the Planck spectrum, by taking $M_S = M_P/2$. As a result, the uncertainties in M_P and n increased by about a factor of 2.